Molecular Photochemistry

International Edition: DOI: 10.1002/anie.201608240
German Edition: DOI: 10.1002/ange.201608240

Luminescent Tungsten(VI) Complexes: Photophysics and Applicability to Organic Light-Emitting Diodes and Photocatalysis

*Kwan-Ting Yeung, Wai-Pong To, Chenyue Sun, Gang Cheng, Chensheng Ma, Glenna So Ming Tong, Chen Yang, and Chi-Ming Che**

Abstract: *The synthesis, excited-state dynamics, and applications of two series of air-stable luminescent tungsten(VI) complexes are described. These tungsten(VI) complexes show phosphorescence in the solid state and in solutions with emission quantum yields up to 22 % in thin film (5 % in mCP) at room temperature. Complex* ***2c****, containing a 5,7-diphenyl-8-hydroxyquinolinate ligand, displays prompt fluorescence (blue–green) and phosphorescence (red) of comparable intensity, which could be used for ratiometric luminescent sensing. Solution-processed organic light-emitting diodes (OLEDs) based on* ***1d*** *showed a stable yellow emission with an external quantum efficiency (EQE) and luminance up to 4.79 % and 1400 cd m^{-2} respectively. These tungsten(VI) complexes were also applied in light-induced aerobic oxidation reactions.*

Although tungsten has been used in incandescent light bulbs for decades, complexes presenting substantial electroluminescence are not reported. As the spin-orbit coupling constant (ζ) of tungsten is comparable to that of iridium and platinum (ζ [cm^{-1}]: 3909 (Ir), 4481 (Pt), and 2433 (W)), tungsten should display a strong heavy atom effect that facilitates intersystem crossing from the singlet excited state to triplet excited state.[1–4] Recently, homoleptic arylisocyanide tungsten(0) and molybdenum(0) complexes were reported to display strong phosphorescence with quantum yields up to 44 % and 2.3 % respectively, but their air-sensitivity might limit material applications.[5] Herein, two new classes of air-stable luminescent tungsten(VI) complexes and their applications in OLEDs and photocatalysis are described. These tungsten(VI) complexes display dominant phosphorescence or dual fluorescence–phosphorescence of comparable intensity, depending on the coordinating ligands.

Figure 1 depicts the structures of **1a–j** and **2a–f** (syntheses and characterization data are given in the Supporting Information, Schemes S1 and S2). Complexes **1i** and **1j** incorporate rigid fluorene moieties into the Schiff base ligand to minimize structural distortion in the emitting excited states.

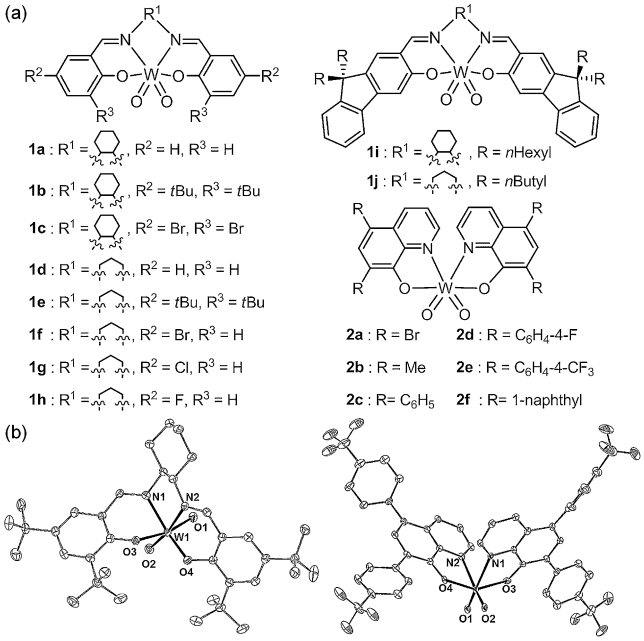

Figure 1. a) Chemical structures of **1a–j** and **2a–f**. b) Perspective views of **1b** (left) and **2e** (right) (Hydrogen atoms are omitted for clarity).

The X-ray crystal structures for **1b**, **1f**, **1g**, and **2e** were determined (Supporting Information, Table S1). All these complexes adopt a distorted octahedral geometry with a *cis*-dioxo unit (Figure 1; Supporting Information). The W–O (oxo) distances range from 1.666 to 1.737 Å.[6–7] For **1b**, **1f**, and **1g**, the Schiff base ligands adopt a β-*cis* geometry with O_p-W-O_p angles of 83.07–86.67° (where O_p = phenolic oxygen atoms). For **2e**, the phenolic oxygen atoms of the quinolinate ligands are *trans* to each other and the two pyridine nitrogen atoms are *trans* to the oxo groups (Figure 1). The N-W-N angles of **1f** and **1g** are 79.06–79.92°, which are larger than that of **1b** (71.56°), presumably because of the flexibility offered by the propylene linkage.

The photophysical data are listed in Table 1 and Table S3 (Supporting Information). Figure 2 displays the absorption and emission spectra for **1a**, **1d**, **1i**, **1j**, and **2a–f**. Complexes **1a–j** and **2a–f** exhibit strong absorption bands at $\lambda < 300$ nm ($\varepsilon = 10.1$–89.2×10^3 M^{-1} cm^{-1}). There are additional strong bands at 310–350 nm ($\varepsilon = 28.2$–29.5×10^3 M^{-1} cm^{-1}) for **1i** and **1j**, attributed to $^1\pi\pi^*$ transitions of the fluorene moieties.

[*] Dr. K.-T. Yeung, Dr. W.-P. To, C. Sun, Dr. G. Cheng, Prof. Dr. C. Ma, Dr. G. S. M. Tong, C. Yang, Prof. Dr. C.-M. Che
State Key Laboratory of Synthetic Chemistry, Institute of Molecular Functional Materials, Department of Chemistry
The University of Hong Kong
Pokfulam Road, Hong Kong SAR (China)
E-mail: cmche@hku.hk
Prof. Dr. C. Ma
School of Chemistry and Chemical engineering, Shenzhen University
Shenzhen 518060 (China)
Dr. G. Cheng, Prof. Dr. C.-M. Che
HKU Shenzhen Institute of Research and Innovation
Shenzhen, Guangdong, 518053 (China)

Supporting information for this article can be found under: http://dx.doi.org/10.1002/anie.201608240.

Table 1: Photophysical data of tungsten(VI) complexes at room temperature.

	Absorption λ_{abs} [nm] (ε [$\times 10^3$ mol^{-1} dm^3 cm^{-1}])[a]	Emission λ_{em} [nm] (τ [µs])[a]	Φ [%][a,b]
1a	243 (sh, 32.1), 271 (sh, 17.8), 301 (sh, 9.4), 345 (sh, 3.0), 400 (3.6)	595 (14.6)	0.3
1b	248 (sh, 20.1), 275 (sh, 14.1), 312 (sh, 6.7), 362 (sh, 2.1), 415 (2.3)	625 (10.0)	0.2
1c	240 (sh, 30.7), 308 (sh, 8.2), 358 (sh, 2.8), 418 (2.9)	618 (16.4)	0.3
1d	243 (35.1), 273 (sh, 17.6), 299 (sh, 12.6), 400 (3.8)	600 (96.9)	2.8
		580[c]	22[c]
1e	245 (22.1), 283 (sh, 11.7), 312 (sh, 8.5), 417 (2.3)	657 (25.7)	0.8
1f	248 (37.6), 297 (sh, 10.1), 413 (3.2)	622 (77.9)	1.6
1g	246 (41.4), 274 (sh, 17.3), 297 (sh, 11.0), 414 (3.7)	623 (56.2)	1.0
1h	244 (23.7), 274 (sh, 12.7), 293 (sh, 8.1), 413 (2.9)	639 (37.2)	1.4
1i	271 (25.0), 312 (sh, 23.6), 330 (sh, 28.6), 349 (29.5), 427 (7.9)	598 (62.0)	2.1
1j	266 (25.1), 327 (29.3), 348 (28.2), 426 (7.7)	600 (16.0)	0.6
2a	263 (47.5), 375 (7.1)	490, 585 (75.9)	0.3
2b	258 (37.5), 385 (4.5)	515, 600 (10.4)	0.1
2c	287 (59.3), 396 (10.5)	515, 614 (42.0)	1.2
2d	284 (62.1), 390 (11.6)	513, 616 (62.0)	0.8
		508, 646[c]	2.5[c]
2e	283 (89.2), 382 (13.4)	501, 602 (25.4)	1.2
2f	262 (43.5), 283 (41.7), 292 (42.0), 383 (9.0)	520, 598 (12.7)	0.4

[a] Dichloromethane solutions. [b] Emission quantum yields (Φ) were measured with $[Ru(bpy)_3][PF_6]_2$ (bpy = 2,2′-bipyridine; $\Phi = 0.062$) in degassed acetonitrile as a standard reference. [c] Absolute emission quantum yields of thin-film samples were measured with a Hamamatsu Quantaurus-QY Absolute PL quantum yields spectrometer C11347. 5 wt% in mCP thin film.

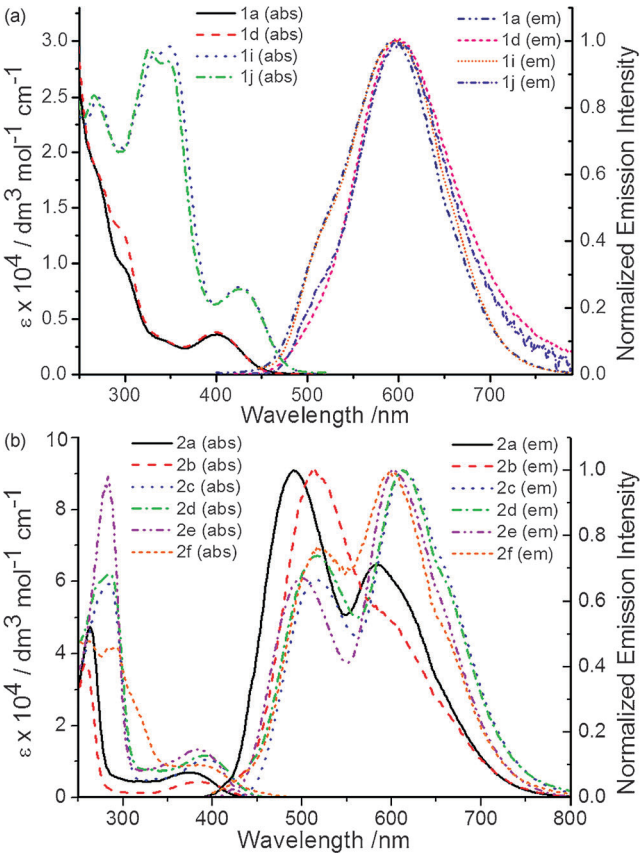

Figure 2. UV/Vis absorption and emission spectra of a) **1a**, **1d**, **1i**, **1j**, and b) **2a–f** at room temperature, measured in degassed dichloromethane solutions.

The lowest energy absorption band for **1a–j** is at 400–427 nm ($\varepsilon = 2.3$–$7.9 \times 10^3\,M^{-1}\,cm^{-1}$) in dichloromethane while for **2a–f** an intense absorption band is observed for each complex at 375–396 nm ($\varepsilon = 4.5$–$13.4 \times 10^3\,M^{-1}\,cm^{-1}$). These low energy absorption bands with high ε values are insensitive to solvent polarity (Supporting Information, Figures S5 and S6) and are assigned to intraligand (IL) transitions. This assignment is consistent with the DFT/TDDFT calculations at the optimized ground state (S_0) geometries (see DFT calculations in the Supporting Information).

All of these complexes display photoluminescence at room temperature (Table 1; Supporting Information, Figure S3) with emission quantum yields (Φ) in the range of 0.1–2.8% in dichloromethane solutions and up to 22% in thin film at room temperature. Complexes **1a–1j** display orange to red emission at 595–657 nm with a shoulder at 500–560 nm in dichloromethane solution (Figure 2; Supporting Information, Figures S7 and S8). The lifetimes of the 595–657 nm emission are in the microsecond regime (10–97 µs) and the radiative decay rate constants (k_r) lie in the range of 1.8–$3.8 \times 10^2\,s^{-1}$. The excitation spectra for **1a–j** agree well with the absorption spectra of the corresponding complexes. Varying the solvent polarity does not induce any significant shift in emission λ_{max} (Supporting Information, Figure S10). The orange–red emission is assigned to a ^{3}IL excited state. In the solid state, the emission blue-shifts to 540–652 nm at 298 K (Supporting Information, Table S3).

For **2a–f**, dual fluorescence–phosphorescence are observed with emission λ_{max} values at 490–520 nm (high energy (HE); $\tau < 0.1$ µs) and at 585–616 nm (low energy (LE); $\tau = 10$–76 µs; Figure 2b). The HE emission band is insensitive to oxygen whereas the LE emission band is strongly quenched under aerated condition (see **2e** in the Supporting Information, Figure S12; see **2c** in Figure 6). This leads to a change in emission color from orange to green. The HE and LE emission bands are assigned to ^{1}IL fluorescence and ^{3}IL phosphorescence of the quinolinolate ligands, respectively. Varying the solvent polarity results in only little change in the wavelength of the HE and LE bands of **2e** (within 400 cm^{-1}; Supporting Information, Figure S11). The HE emission is more intense than the LE emission when there is no aryl substituent on the quinolinolate (Qin) ligand (**2a** and **2b**) but the trend is reversed for **2c–2f** when the Qin ligand has aryl substituents on the 5- and 7-position.

The emission properties of **1d** and **2d** in thin films have been examined. The emission maximum of **1d** in 1,3-bis(carbazol-9-yl)benzene (mCP) thin film (5 wt%) is at 580 nm and is insensitive to complex concentration; the

emission quantum yield is 22% at room temperature (Supporting Information, Figure S13). For **2d**-doped mCP thin film, two emission maxima at approximately 504–508 nm (HE) and approximately 642–650 nm (LE) are observed.

DFT/TDDFT calculations were performed to shed light on the effect of auxiliary ligand on the intersystem crossing (ISC) efficiency. For facile ISC, the presence of a close-lying triplet excited state (T_n) relative to the singlet excited state (usually the first singlet excited state, S_1), with a small $|\Delta E(S_1-T_n)|$, is crucial. Figure 3 depicts an energy level diagram for the relative energies of the S_1 and the closest triplet excited state for **1a**, **1d**, **2b**, and **2e** at their respective optimized S_0 geometries. The triplet excited states (which happened to be the T_3 excited state for all complexes investigated) lying closest to the S_1 excited state of **1a** and **1d** are 790 and 573 cm^{-1} below the S_1 excited state, respectively; on the other hand, the T_3 excited state is 1770 and 1612 cm^{-1} above the S_1 excited state for **2b** and **2e**, respectively. Thus, ISC efficiency correlates well with the singlet–triplet energy gap ($|\Delta E(S_1-T_3)|$).

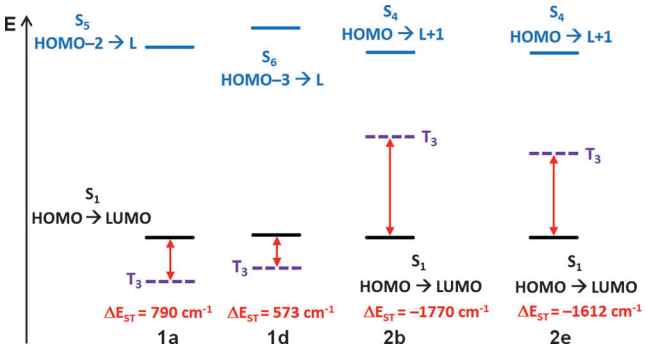

Figure 3. Energy level diagrams for **1a**, **1d**, **2b**, and **2e**. The singlet excited states (blue solid line) and triplet excited states (purple dashed lines) are of the same parentage. A negative sign in ΔE_{ST} means that the S_1 excited state is below the T_3 excited state.

Figure 4 and Figure S14 (Supporting Information) respectively depict the evolutions of femtosecond time-resolved fluorescence (fs-TRF) and the corresponding decays of the emission intensities for **1i** and **2d**. Photoexcitation at 350 nm in dichloromethane solution results in broad and structureless prompt fluorescence (PF) with an emission peak at $\lambda_f \approx 530$ nm (**1i**, Figure 4a) and approximately 515 nm (**2d**, Figure S14), which coincides with that of the shoulder for **1i** and the HE band for **2d** in their respective steady-state luminescence spectra. The PF decay time constants (τ_f), attributed to the ISC of the S_1 excited state to the triplet manifold (T_n), are 64, 52, and 42 ps for **1a**, **1d**, and **1i**, respectively, and 110, 102, and 93 ps for **2b**, **2d**, and **2e**, respectively; the Schiff base complexes generally have a faster ISC efficiency than the quinolinolate complexes.

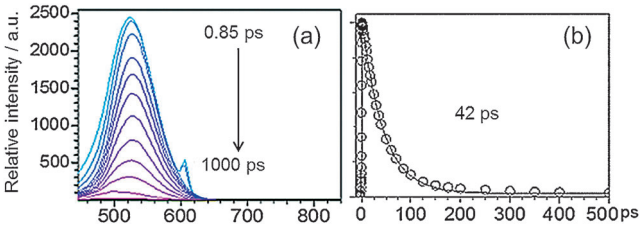

Figure 4. a) Temporal evolution and b) experimental (○) and fitted (lines) intensity decay profiles of fs-TRF for **1i** in dichloromethane upon photoexcitation at $\lambda_{exc} = 350$ nm.

Figure 5 and Figures S15–18 (Supporting Information) display the frontier molecular orbital (MO) surfaces of **1a**, **1d**, **2b**, and **2e**. For **1a** and **1d**, the S_1 excited state is mainly derived from a HOMO→LUMO transition and the closest T_3 excited state has a significant contribution from the H-2 (H-3)→LUMO transition for **1a** (**1d**). The singlet counterpart of the T_3 excited state is S_5 for **1a** and S_6 for **1d**. Owing to the longer bridging alkyl chain in **1d**, the angle between the two phenolic moieties of **1a** and **1d** are approximately 68° and 82°, respectively. As the two phenolic moieties are in a nearly orthogonal conformation in **1d**, both HOMO and H-3 are mainly localized on one of the phenolic moieties (>90%; Figure 5a). On the other hand, as the angle is smaller in **1a**, there is electron density on both phenolic moieties in the H-2 of **1a** (74 and 14%; Supporting Information, Figure S15), thus destabilizing the H-2 of **1a** relative to H-3 of **1d**. In effect, the energy gap between the HOMO and H-2 of **1a** is smaller than the corresponding gap between the HOMO and H-3 of **1d**. Moreover, because of the localized nature of the relevant orbitals, the S_6–T_3 energy gap of **1d** and the S_5–T_3 energy gap of **1a** are comparatively large. As a consequence, the S_1–T_3 energy gap for both **1a** and **1d** is small and the T_3 excited state is below the S_1 excited state. Furthermore, as the relevant MOs are more localized for **1d**, the T_3 excited state is closer in energy to the S_1 excited state for **1d** than for **1a** (Figure 3). Hence, **1d** has a faster ISC rate, which is consistent with the experimental findings.

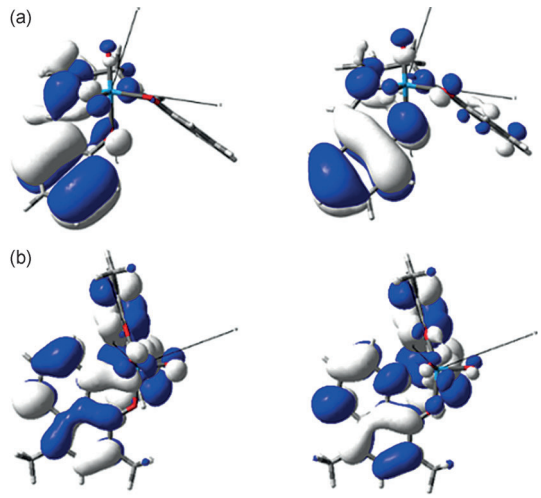

Figure 5. a) HOMO (right) and H-3 (left) for **1d**. b) LUMO (left) and L+1 (right) for **2b**.

The S_1 excited states for **2b** and **2e** are also derived from a HOMO→LUMO transition but the triplet excited state lying closest to the S_1 excited state, T_3, is derived from a HOMO→L+1 transition and the singlet counterpart of T_3

is S_4. As shown in Figure 5b and Figures S17 and S18 (Supporting Information), both the HOMO and L + 1 orbitals are delocalized over the two Qin ligands, resulting in a small $\Delta E(S_4-T_3)$ energy gap (< 2000 cm^{-1}). On the other hand, $\Delta E(S_4-S_1)$ is more than 3500 cm^{-1}; hence, the T_3 excited state is more than 1600 cm^{-1} above the S_1 excited state. (Figure 3). For **2e** with aryl substituents at the Qin ligand, the frontier orbitals are more delocalized, leading to more mixing among different transitions and a larger $\Delta E(S_4-T_3)$ energy gap (Supporting Information). Thus, $|\Delta E(S_1-T_3)|$ is smaller and the ISC rate of **2e** is faster than **2b**.

Application studies of these tungsten(VI) complexes are described below. Complex **2c** acted as a ratiometric sensor for dissolved oxygen.[8] As shown in Figure 6, the phosphorescence of **2c** decreased upon diffusion of air into the solution while the fluorescence remained unchanged. The emission color gradually changed from orange to green.

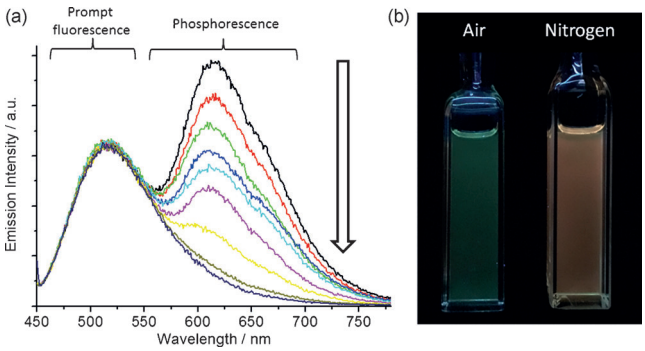

Figure 6. a) Emission spectral change of **2c** in dichloromethane upon diffusion of air into the solution. The arrow indicates the change in emission intensity. b) Photo showing the emission of a dichloromethane solution of **2c** (5×10^{-5} M) under air and nitrogen, respectively (λ_{exc} = 365 nm).

Solution-processed OLEDs were fabricated to examine the electroluminescence (EL) properties of the tungsten(VI) complexes using **1d** as an example (details in the Supporting Information). 2,6-dicarbazolo-1,5-pyridine (PYD2) was used as the host. As depicted in Figure 7a, EL spectra of the **1d** device displayed a broad structureless emission with a maximum at 577 nm and CIE chromaticity coordinates of (0.46, 0.50). Such emission was similar to the PL of **1d** in mCP thin film (Supporting Information, Figure S13), suggesting efficient energy transfer from the PYD2 host to the tungsten emitter. EQE-luminance characteristics of these devices (Figure 7b) showed a maximum EQE of 4.79% for the device with 4 wt% **1d** at a luminance of approximately 40 cd m^{-2}. High luminance up to 1400 cd m^{-2} was realized for the device with 2 wt% **1d**. To our knowledge, this is the first realization of a molecular tungsten OLED device.

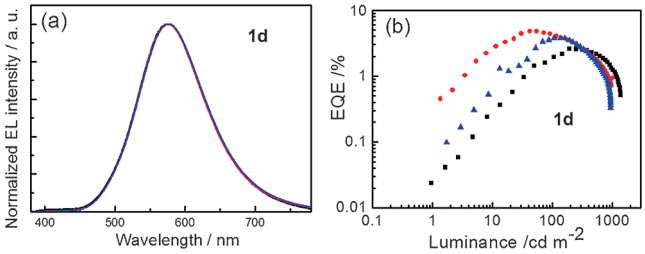

Figure 7. a) Normalized EL spectra (2 wt% (——), 4 wt% (——), 6 wt% (——)) and b) EQE-luminance characteristic of OLEDs based on **1d** with 2 wt% (■), 4 wt% (●), and 6 wt% (▲) dopant concentrations.

The photocatalytic activity of **1i** and **2c** using light-induced cyanation of tertiary amines as examples, has been examined (Scheme 1; Supporting Information, Tables S5 and S6). Their excited-state reduction potentials $E(W^*/W^-)$ are estimated to be 0.59 and 0.40 V versus $Cp_2Fe^{+/0}$, respectively. Both **1i** and **2c** (2 mol%) were found to catalyze the formation of α-aminonitriles in good to excellent yields (77–88% with **1i**; 78–95% with **2c**) under $\lambda > 370$ nm light irradiation. Singlet oxygen sensitized by the triplet-excited tungsten(VI) complex is proposed to be the active oxidant.[9] Besides, aerobic oxidative hydroxylation of aryl boronic acids to aryl alcohols using **2c** as photocatalyst has also been demonstrated.[10] Irradiation ($\lambda > 370$ nm) of a mixture of aryl boronic acids, **2c** (1 mol%), and diisopropylethylamine in DMF, afforded the respective aryl alcohols with yields of 57–82% in three hours. These examples reveal the potentially rich photochemistry of luminescent tungsten(VI) complexes.

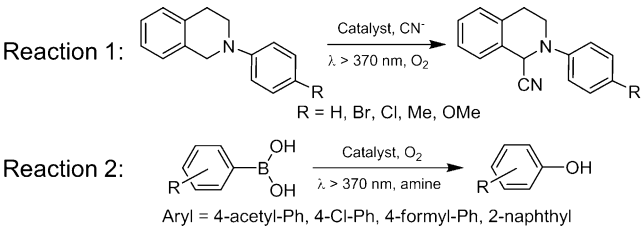

Scheme 1. Reaction 1) Oxidative cyanation of tertiary amines photocatalyzed by **1i** and **2c**. Reaction 2) Oxidative hydroxylation of aryl boronic acids photocatalyzed by **2c**.

In summary, we have realized the feasibility of developing air-stable luminescent tungsten(VI) complexes with room temperature emission quantum yields reaching 22%. Changing the supporting ligand allows modulation of ISC efficiency and dual fluorescence–phosphorescence with comparable intensities has been realized. It is conceivable that air-stable phosphorescent tungsten complexes, such as the tungsten(VI) species described herein, could become as competitive as other luminescent complexes of iridium(III) and platinum(II).[11] The absence of a deactivating d-d ligand field excited state in tungsten(VI) may provide an advantage over other metal complexes when materials with high-energy phosphorescence are desired.

Acknowledgements

This work was supported by the Theme-Based Research Scheme (Project No. T23-713/11), the Innovation and Technology Commission of the HKSAR Government (ITS/140/16), Guangdong Special Project of the Introduction

of Innovative R&D Teams and GuangDong Aglaia Optoelectronic Materials Co., Ltd., and Basic Research Program of Shenzhen (JCYJ20160229123546997, JCYJ20160530184056496). This work was also conducted in part using the research computing facilities and/or advisory services offered by Information Technology Services, the University of Hong Kong. KTY acknowledges the receipt of a postgraduate studentship from The University of Hong Kong.

Conflict of interest

The authors declare no conflict of interest.

Keywords: dual fluorescence–phosphorescence · organic light-emitting devices · phosphorescence · photocatalysis · tungsten

[1] a) M. Wrighton, G. S. Hammond, H. B. Gray, *J. Am. Chem. Soc.* **1971**, *93*, 4336; b) M. Wrighton, G. S. Hammond, H. B. Gray, *Inorg. Chem.* **1972**, *11*, 3122; c) A. J. Lees, A. W. Adamson, *J. Am. Chem. Soc.* **1980**, *102*, 6874; d) K. A. Rawlins, A. J. Lees, S. J. Fuerniss, K. I. Papathomas, *Chem. Mater.* **1996**, *8*, 1540.

[2] M. C. Manning, W. C. Trogler, *J. Am. Chem. Soc.* **1983**, *105*, 5311.

[3] a) A. B. Bocarsly, R. E. Cameron, H.-D. Rubin, G. A. McDermott, C. R. Wolff, A. Mayr, *Inorg. Chem.* **1985**, *24*, 3976; b) R. E. Da Re, M. D. Hopkins, *Coord. Chem. Rev.* **2005**, *249*, 1396.

[4] a) T. C. Zietlow, D. G. Nocera, H. B. Gray, *Inorg. Chem.* **1986**, *25*, 1351; b) A. W. Maverick, J. S. Najdzionek, D. MacKenzie, D. G. Nocera, H. B. Gray, *J. Am. Chem. Soc.* **1983**, *105*, 1878.

[5] a) W. Sattler, L. M. Henling, J. R. Winkler, H. B. Gray, *J. Am. Chem. Soc.* **2015**, *137*, 1198; b) W. Sattler, M. E. Ener, J. D. Blakemore, A. A. Rachford, P. J. LaBeaume, J. W. Thackeray, J. F. Cameron, J. R. Winkler, H. B. Gray, *J. Am. Chem. Soc.* **2013**, *135*, 10614; c) L. A. Büldt, X. Guo, A. Prescimone, O. S. Wenger, *Angew. Chem. Int. Ed.* **2016**, *55*, 11247; *Angew. Chem.* **2016**, *128*, 11413.

[6] A. Thapper, O. Balmes, C. Lorber, P. H. Svensson, R. H. Holm, E. Nordlander, *Inorg. Chim. Acta* **2001**, *321*, 162.

[7] a) Y.-L. Wong, Y. Yan, E. S. H. Chan, Q. Yang, T. C. W. Mak, D. K. P. Ng, *J. Chem. Soc. Dalton Trans.* **1998**, 3057; b) Y.-L. Wong, J.-F. Ma, W.-F. Law, Y. Yan, W.-T. Wong, Z.-Y. Zhang, T. C. W. Mak, D. K. P. Ng, *Eur. J. Inorg. Chem.* **1999**, 313; c) Y.-L. Wong, L. H. Tong, J. R. Dilworth, D. K. P. Ng, H. K. Lee, *Dalton Trans.* **2010**, *39*, 4602.

[8] a) T. Yoshihara, Y. Yamaguchi, M. Hosaka, T. Takeuchi, S. Tobita, *Angew. Chem. Int. Ed.* **2012**, *51*, 4148; *Angew. Chem.* **2012**, *124*, 4224; b) F.-F. Hung, W.-P. To, J.-J. Zhang, C. Ma, W.-Y. Wong, C.-M. Che, *Chem. Eur. J.* **2014**, *20*, 8604; c) J. Lehr, M. Tropiano, P. D. Beer, S. Faulkner, J. J. Davis, *Chem. Commun.* **2015**, *51*, 15944; d) Q. Zhao, X. Zhou, T. Cao, K. Y. Zhang, L. Yang, S. Liu, H. Liang, H. Yang, F. Li, W. Huang, *Chem. Sci.* **2015**, *6*, 1825.

[9] a) M. C. DeRosa, R. J. Crutchley, *Coord. Chem. Rev.* **2002**, *233*, 351; b) W.-P. To, Y. Liu, T.-C. Lau, C.-M. Che, *Chem. Eur. J.* **2013**, *19*, 5654; c) P. K. Chow, C. Ma, W.-P. To, G. S. M. Tong, S.-L. Lai, S. C. F. Kui, W.-M. Kwok, C.-M. Che, *Angew. Chem. Int. Ed.* **2013**, *52*, 11775; *Angew. Chem.* **2013**, *125*, 11991.

[10] Y.-Q. Zou, J.-R. Chen, X.-P. Liu, L.-Q. Lu, R. L. Davis, K. A. Jørgensen, W.-J. Xiao, *Angew. Chem. Int. Ed.* **2012**, *51*, 784; *Angew. Chem.* **2012**, *124*, 808.

[11] a) H. Yersin, A. F. Rausch, R. Czerwieniec, T. Hofbeck, T. Fischer, *Coord. Chem. Rev.* **2011**, *255*, 2622; b) C. Fan, C. Yang, *Chem. Soc. Rev.* **2014**, *43*, 6439; c) X. Yang, G. Zhou, W.-Y. Wong, *Chem. Soc. Rev.* **2015**, *44*, 8484; d) K. Li, G. S. M. Tong, Q. Wan, G. Cheng, W.-Y. Tong, W.-H. Ang, W.-L. Kwong, C.-M. Che, *Chem. Sci.* **2016**, *7*, 1653.

Manuscript received: August 23, 2016
Final Article published: ■■ ■■, ■■■■

Communications

Molecular Photochemistry

K.-T. Yeung, W.-P. To, C. Sun, G. Cheng, C. Ma, G. S. M. Tong, C. Yang, C.-M. Che* _____ ▮▮▮▮–▮▮▮▮

Luminescent Tungsten(VI) Complexes: Photophysics and Applicability to Organic Light-Emitting Diodes and Photocatalysis

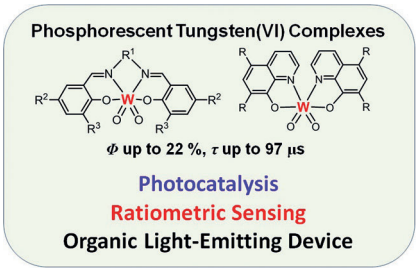

Luminescent tungsten complexes were realized by coordination of polydentate ligands to a tungsten metal center. These metal complexes exhibit interesting photophysical and photocatalytic properties with intense phosphorescence at room temperature and dual fluorescence–phosphorescence covering the entire spectrum. They are capable phosphorescent dopants for solution-processable organic light-emitting diodes.

